Published OnlineFirst July 7, 2016; DOI: 10.1158/1940-6207.CAPR-16-0066

Research Article

Cancer Prevention Research

AKT1 Activation is Obligatory for Spontaneous BCC Tumor Growth in a Murine Model that Mimics Some Features of Basal Cell Nevus Syndrome

Arianna L. Kim[1], Jung Ho Back[1], Yucui Zhu[1], Xiuwei Tang[1], Nathan P. Yardley[1], Katherine J. Kim[1], Mohammad Athar[2], and David R. Bickers[1]

Abstract

Patients with basal cell nevus syndrome (BCNS), also known as Gorlin syndrome, develop numerous basal cell carcinomas (BCC) due to germline mutations in the tumor suppressor *PTCH1* and aberrant activation of Hedgehog (Hh) signaling. Therapies targeted at components of the Hh pathway, including the smoothened (SMO) inhibitor vismodegib, can ablate these tumors clinically, but tumors recur upon drug discontinuation. Using SKH1-*Ptch1*$^{+/-}$ as a model that closely mimics the spontaneous and accelerated growth pattern of BCCs in patients with BCNS, we show that AKT1, a serine/threonine protein kinase, is intrinsically activated in keratinocytes derived from the skin of newborn *Ptch1*$^{+/-}$ mice in the absence of carcinogenic stimuli. Introducing *Akt1* haplodeficiency in *Ptch1*$^{+/-}$ mice (*Akt1*$^{+/-}$ *Ptch1*$^{+/-}$) significantly abrogated BCC growth. Similarly, pharmacological inhibition of AKT with perifosine, an alkyl phospholipid AKT inhibitor, diminished the growth of spontaneous and UV-induced BCCs. Our data demonstrate an obligatory role for AKT1 in BCC growth, and targeting AKT may help reduce BCC tumor burden in BCNS patients. *Cancer Prev Res; 9(10); 794–802. ©2016 AACR.*

Introduction

Hedgehog (Hh) pathways are crucial for vertebrate fetal development (1). Of the three known mammalian Hh ligands, Sonic hedgehog (SHH) regulates segment polarity as well as a wide range of biological activities, from establishing left–right body symmetry and limb patterning to eye and central nervous system development. The other two Hh ligands, Desert hedgehog (DHH) and Indian hedgehog (IHH), are mainly involved in the development of male germ cells and cartilage, respectively (1). In the absence of SHH, PTCH1, a tumor suppressor and the Hh receptor, blocks Hh signaling by repressing a membrane-bound, G-protein–coupled, receptor-like protein known as smoothened (SMO) (1, 2). The binding of SHH to PTCH1 relieves SMO repression, triggering a canonical Hh response whereby SMO moves to the primary cilium, and activates the GLI family of transcription factors (3). GLI forms a cytoplasmic complex with several accessory modulators, including the serine–threonine kinase Fused (FU), Suppressor of Fused (SUFU), and costal2 (COS2), a kinesin-related protein that binds the GLI-containing complex to microtubules. It is believed that SMO activity favors dissociation of these complexes and translocation of an active form of GLI from the cytoplasm to the nucleus, where it promotes the transcription of Hh target genes, including *PTCH1*, *GLI*, *CCND1*, bone morphogenic proteins (BMPs), and a member of the TGFβ superfamily (1, 2, 4).

The Hh pathway while highly active during human fetal development normally shuts down soon after birth. However, aberrant activation in adults drives the development and/or maintenance of numerous types of human malignancies, including cancers of the pancreas, prostate, and brain. It also regulates the proliferation of cancer stem cells (CSC), tumor progression, and metastases and may also hasten tumor relapse by augmenting multidrug resistance (MDR) pathways (2, 5). While most human tumors do not harbor somatic mutations in the Hh signaling pathway and demonstrate ligand-dependent Hh pathway activation (6), ligand-independent Hh pathway activation underlies the development of basal cell carcinoma (BCC), the most common type of human malignancy wordwide, due to loss-of-function mutations in *PTCH1*, gain-of-function mutations in *SMO*, as well as missense mutations in *GLI1* and *GLI3* (7). Germline mutations in *PTCH1* cause basal cell nevus syndrome (BCNS) or Gorlin syndrome (8). Individuals affected with BCNS typically develop large numbers of BCCs often beginning in early chilhood and are at substantially increased risk for additional neoplasms such as medulloblastomas and rhabdomyosarcomas. The clinical utility of targeting aberrant Hh signaling in BCNS patients is illustrated by the results of our phase II clinical trial that showed that the orally administered SMO inhibitor vismodegib had remarkable efficacy in ablating BCCs (9). While these and other successes led to FDA approval of vismodegib for treating advanced/inoperable and metastatic BCCs, subsequent studies revealed significant tumor recurrence and acquired clinical resistance to vismodegib. This occurs during therapy primarily through secondary mutations in *SMO* (for example, D473G, D473Y, Q477E, and G497W) and, to a lesser extent, through concurrent copy number changes in *SUFU* and *GLI2*, thereby impairing drug binding and/or

[1]Department of Dermatology, Columbia University Medical Center, New York, New York. [2]University of Alabama at Birmingham, Birmingham, Alabama.

Corresponding Authors: Arianna L. Kim, Columbia University Medical Center, 1150 St. Nicholas Avenue 318A, New York, NY 10032. Phone: 212-851-4541; Fax: 212-851-4540; E-mail: ak309@cumc.columbia.edu; and David R. Bickers, drb25@cumc.columbia.edu.; Mohammad Athar, mathar@uabmc.edu

doi: 10.1158/1940-6207.CAPR-16-0066

Published OnlineFirst July 7, 2016; DOI: 10.1158/1940-6207.CAPR-16-0066

reactivating Hh pathways, confirming the importance of the Hh pathway in BCC growth (10–13). Several lines of evidence, however, demonstrate that additional pathways may synergistically contribute to BCC tumor growth. For example, there is a high risk of BCC in patients with cartilage-hair hypoplasia (CHH), an inherited disorder due to mutations in the *RMRP* (RNA component of mitochondrial RNA-processing endoribonuclease), and in patients with xeroderma pigmentosum (XP), an autosomal recessive disorder with defective nuclear excision DNA repair (14). Recently, a significant fraction of human BCCs was shown to carry mutations in various cancer-related genes that regulate a variety of cellular processes, including cell growth, differentiation, mitotic cycle, and oncogenic transformation (15). These data implicate involvement of multiple tumor driver pathways in BCC pathogenesis and suggest that identification of molecular targets distinct from SMO could help ameliorate the limitations of currently available SMO inhibitors and improve therapeutic index. One such molecular target that we have identified is AKT1, the serine/threonine protein kinase that regulates cell survival and is known to be dysregulated in numerous types of human cancer (16–20). Using SKH1-1-*Ptch1*$^{+/-}$ mice that we recently described as a susceptible model for BCCs development, this study demonstrates that AKT1 is obligatory for BCC tumorigenesis, and that genetic and pharmacological inhibition of AKT prevents BCC growth.

Materials and Methods

Cells and reagents

Adult normal human epidermal keratinocytes (Lonza) and murine ASZ001 BCC cells (a gift from Dr. E. Epstein Jr.; ref. 21) were cultured in Medium 154CF, supplemented with Human Keratinocyte Growth Supplement (Thermo Fisher). ASZ001 cells display cellular morphology similar to that of human BCCs, express BCC markers, and are sensitive to SMO inhibition (22, 23). The authors did not authenticate the cell lines. pUSEamp-*myrAkt1* was obtained from Millipore. Perifosine was purchased from Selleckchem, edelfosine from Sigma-Aldrich, and MK-2206 from ChemieTek.

Western blotting, immunohistochemistry, and immunofluorescence

The experiments were performed as previously described (24–26). Antibodies against AKT1, AKT2, AKT3, p-AKT1 (S473), GLI1, and GLI2 were purchased from Cell Signaling Technology, SOX9 from Abcam, and β-actin from Sigma-Aldrich. Fluorescent images were acquired using the Zeiss LSM 5 Exciter confocal microscope with 40× oil immersion objective (Carl Zeiss) and analyzed using ImageJ software (NIH).

Proliferation assay

Proliferation was assessed using BrdUrd kit III (Roche Diagnostics Corp.), and Click-iT Plus EdU Alexa Fluor 488 Imaging Kit (Thermo Fisher) according to the manufacturers' instructions.

Colony formation assay

Primary human keratinocytes were transduced with the viral construct expressing *myrAkt1* (pUSEamp-*myrAkt1*) or pUSEamp vector (Millipore) at 10 μg using lipofectamine 2000 (Invitrogen) and stable colonies were selected in the presence of G418 (Sigma-Aldrich). Virally transduced cells were then irradiated with UV (30 mJ/cm^2). Cells were then resuspended in top agar (0.7% agarose in keratinocyte media) and placed with the base layer prepared in 0.8% agar in keratinocyte media with supplements. After 3 weeks, cells were stained with Crystal Violet, and the number of colonies was counted. The experiment was repeated twice independently.

Generation of SKH1-*Ptch1*$^{+/-}$ and SKH1-*Akt1*$^{+/-}$ *Ptch1*$^{+/-}$ mice and assessment of microscopic lesions

All animal experiments were performed in accordance with guidelines of our approved Columbia University Institutional Animal Care and Use Committee (IACUC) protocol. SKH1-*Ptch1*$^{+/-}$ mice were generated by crossing B6-*Ptch1*$^{+/-}$ (27) with SKH1 hairless mice (Charles River Laboratories). The resulting haired *Ptch1*$^{+/-}$ F1 littermates were backcrossed for 10 generations to generate SKH1-*Ptch1*$^{+/-}$ mice. SKH1-*Akt1*$^{+/-}$ *Ptch1*$^{+/-}$ mice were generated by crossing B6.129P2-Akt1tm1Mbb/J mice (Jackson Lab) with SKH1-*Ptch1*$^{+/-}$ mice. The resulting haired *Akt1*$^{+/-}$ *Ptch1*$^{+/-}$ F1 littermates were backcrossed for 10 generations to generate SKH1-*Akt1*$^{+/-}$ *Ptch1*$^{+/-}$ mice. Tissue samples were prepared from H&E- and β-gal–stained full-thickness dorsal skin. For β-gal staining, glutaraldehyde and formalin-fixed tissues were treated with X-gal and iron buffer solution (Roche Diagnostics Corp.) for 48 hours and were processed using the manufacturer's protocol. Microscopic BCC-like lesions were defined as tumor islands composed of monomorphic basaloid cells with scant cytoplasm arranged as nests within the dermis. These lesions were counted as numbers per unit area and as total tumor area per square millimeter skin section as previously described (28). For each mouse, three skin strips (average 1.5 cm × 0.1 cm) were analyzed.

UV light source

A UV Irradiation Unit (Daavlin Co.) equipped with an electronic controller to regulate dosage was used. The UV source consisted of eight FS72T12-UV-HO lamps that emit UV (290–320 nm, 75%–80% of total energy) and UVA (320–380 nm, 20%–25% of total energy). A UVC sensor (Oriel's Goldilux UVC Probe) was routinely used during each exposure to confirm lack of UVC emission. The dose of UV was quantified with a UV Spectrum 305 Dosimeter obtained from the Daavlin Co. The radiation was further calibrated with an IL1700 Research Radiometer/Photometer from International Light Inc.

Tumor protocol in *Ptch1*$^{+/-}$ and *Akt1*$^{+/-}$ *Ptch1*$^{+/-}$ mice

UV study: *Ptch1*$^{+/-}$ and *Akt1*$^{+/-}$ *Ptch1*$^{+/-}$ and their wild-type *Ptch1*$^{+/+}$ littermates were irradiated with UV (180 mJ/cm^2 twice per week for 30 weeks). *Itraconazole study*: *Ptch1*$^{+/-}$ mice ($n = 20$) were UV-irradiated (180 mJ/cm^2 twice per week for 30 weeks) to induce BCCs. Irradiation was terminated. Mice were then treated with 2-hydroxypropyl-b-cyclodextrin ($n = 10$) or itraconazole ($n = 10$) (Sigma-Aldrich) (twice daily, 100 mg/kg, i.p.) for 24 days. The size of tumors was measured as previously described (28). For the perifosine study, control group received 0.9% NaCl/100 μL (gavage) ($n = 8$), while the experimental group received perifosine (125 mg/kg body weight prepared in 0.9% NaCl, gavage, twice a week, $n = 8$) 30 minutes prior to each UV irradiation. All animals were irradiated with 180 mJ/cm^2 UV twice weekly for 32 weeks. Tumor number and tumor volume were recorded once a week and plotted in terms of weeks on test.

Published OnlineFirst July 7, 2016; DOI: 10.1158/1940-6207.CAPR-16-0066

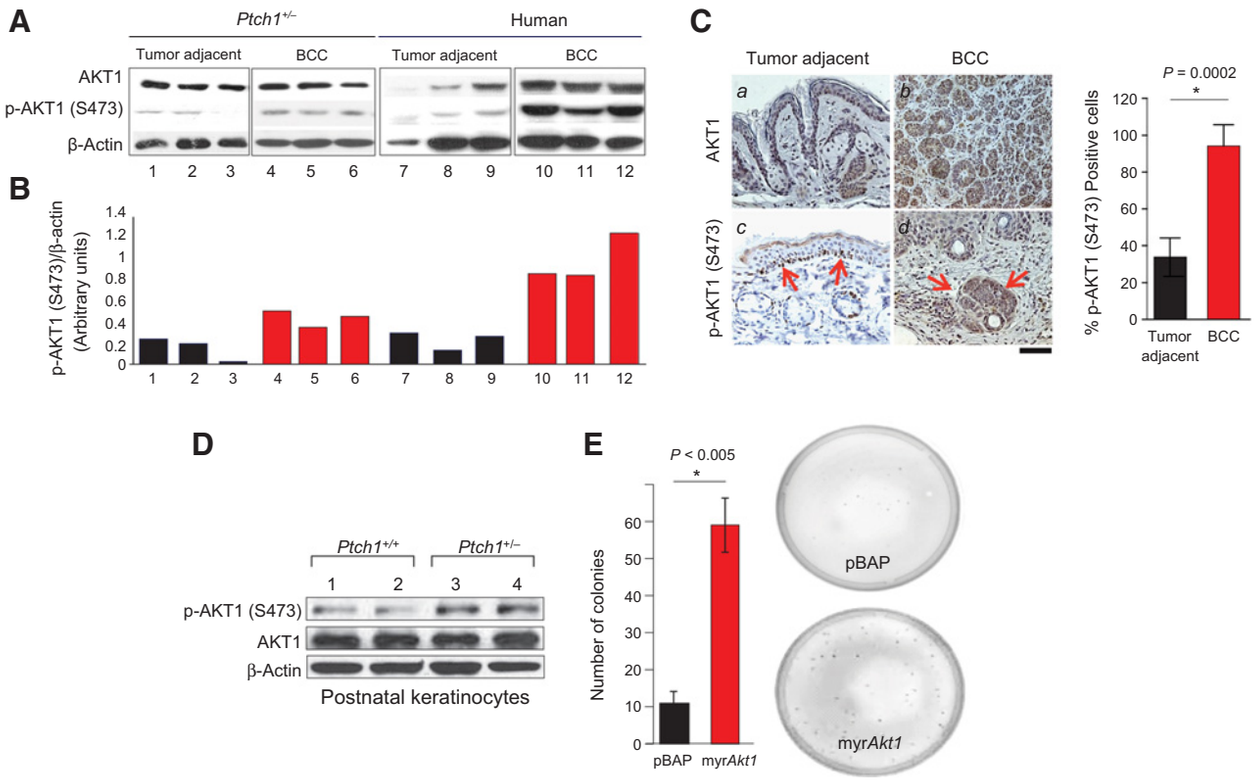

Figure 1.

AKT1 is intrinsically activated in *Ptch1*$^{+/-}$ keratinocytes and spontaneous BCCs. **A,** the levels of p-AKT1 (S473) in spontaneous murine BCCs developed in SKH1-*Ptch1*$^{+/-}$(*Ptch1*$^{+/-}$) mice and human BCCs. Western blotting assessed three representative BCCs from three different animals or three separate patients. β-Actin was used as an internal control. **B,** densitometric scanning of **A**. **C,** immunohistochemical assessment of AKT1 and p-AKT1 (S473) in tumor adjacent skin (a, c) and spontaneous BCCs (b, d) in *Ptch1*$^{+/-}$mice. Scale bar, 100 μm. Histogram represents percent p-AKT1 (S473)-positive cells in tumor-adjacent skins and BCCs in *Ptch1*$^{+/-}$mice. Three fields were counted. *, $P < 0.05$. **D,** p-AKT S473 levels are increased in primary keratinocytes isolated from postnatal day 2 *Ptch1*$^{+/-}$ mice (lanes 3 and 4), but not in primary keratinocytes isolated from postnatal day 2 WT *Ptch1*$^{+/+}$ mice (lanes 1 and 2). **E,** increased colony-forming capability of normal human keratinocytes expressing constitutively active AKT1 (pUSEamp-*myrAkt1, myrAkt1*). *, $P < 0.005$, compared with control. Normal primary human keratinocytes were transduced either with a viral construct expressing myr-*Akt1* (myr-*Akt1*) or vector (-, pBAP) only.

Statistical analyses

Statistical analyses were performed using the Student *t* test (two-tailed): $P < 0.05$ was considered statistically significant.

Results

AKT1 is intrinsically activated in *Ptch1*$^{+/-}$ keratinocytes and spontaneous BCCs

We recently showed that the growth of BCC is greatly enhanced in hairless SKH1-*Ptch1*$^{+/-}$ mice (26). Although the original introduction of *Ptch1*$^{+/-}$ into the C57BL/6 strain (B6-*Ptch1*$^{+/-}$; ref. 27) rendered these animals susceptible to BCC following skin exposure to ionizing or UV radiation (29), these tumors grow quite slowly in these mice—perhaps due to their derivation from the C57BL/6 genetic background that is known to be inherently tumor resistant. In contrast, SKH1 hairless mice are highly susceptible to the growth of squamous cell carcinomas (SCC) following chronic UV exposure (25, 30). Chronic UV irradiation of SKH1-*Ptch1*$^{+/+}$ wild-type (WT) mice results in the sequential growth of benign papillomas and SCCs in a pattern closely mimicking that of human SCCs, while these animals never develop BCCs. By introducing *Ptch1* heterozygosity onto the tumor-susceptible SKH1 hairless background, we generated SKH1-*Ptch1*$^{+/-}$ (hereafter referred to as *Ptch1*$^{+/-}$) mice. These animals exhibit the spontaneous growth of BCCs that characterizes patients with BCNS (31). AKT activation typically occurs in response to extracellular stimuli, and its phosphorylation at S473 is necessary for the full activation of the PI3K–AKT pathway (32). We detected S473 phosphorylation in BCCs that developed spontaneously in *Ptch1*$^{+/-}$ mice and in human BCCs (Fig. 1A and B). AKT S473 phosphorylation was present in tumor cells but was undetectable in tumor stroma (Fig. 1C). Moreover, AKT S473 phosphorylation was detectable in primary keratinocytes isolated from newborn *Ptch1*$^{+/-}$, suggesting that AKT activation occurs in the absence of external stimuli in these cells (Fig. 1D). To confirm the role of AKT1 in cell survival and proliferation, we force activated AKT1 by transfecting myristoylated *Akt1* (myr-*Akt1*) into normal human primary keratinocytes. This resulted in enhanced colony formation (Fig. 1E). Together, these data suggest that the concurrent activation of both AKT and Hh pathways may play a crucial role in promoting BCC growth.

Published OnlineFirst July 7, 2016; DOI: 10.1158/1940-6207.CAPR-16-0066

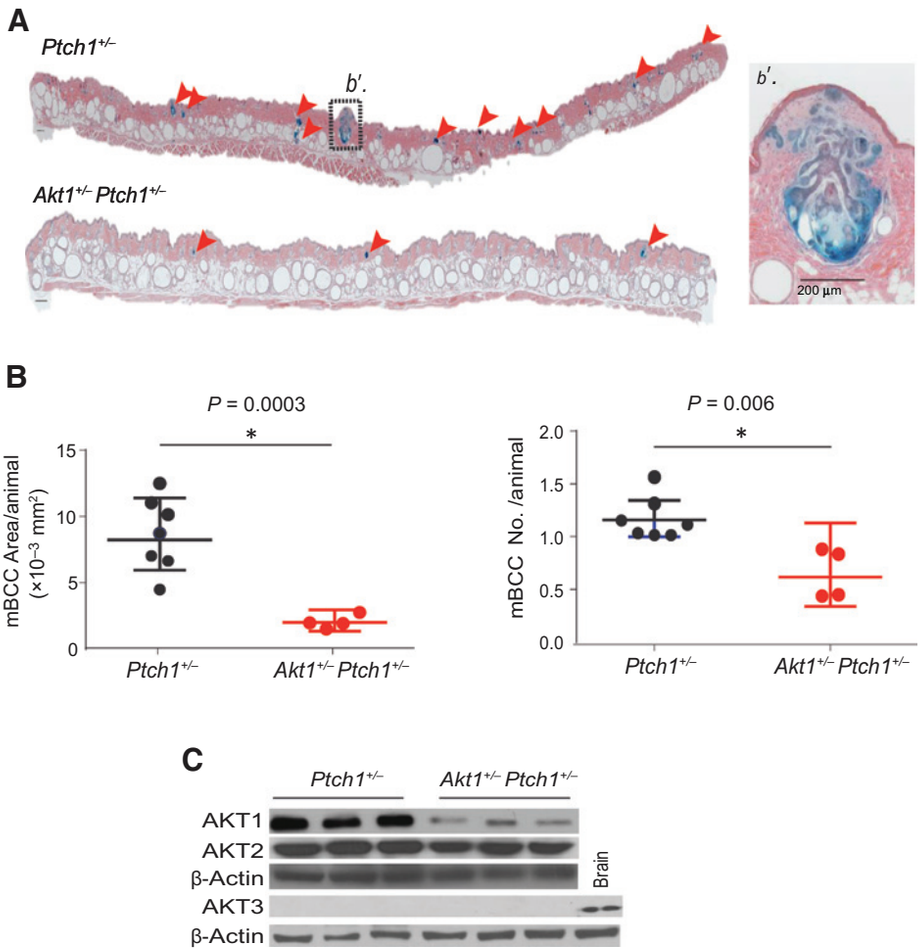

Figure 2.
Akt1 haplodeficiency is sufficient to prevent the growth of spontaneous microscopic BCCs. **A,** representative H&E staining of skin sections from *Akt1*$^{+/-}$ *Ptch1*$^{+/-}$ mice and *Ptch1*$^{+/-}$ littermates. Scale bar, 200 μm. **B,** assessment of size and number of spontaneous BCCs in *Akt1*$^{+/-}$ *Ptch1*$^{+/-}$ and *Ptch1*$^{+/-}$. Three skin strips (average 1.5 cm × 0.1 cm) were analyzed for each mouse. Each dot represents data from one mouse. **C,** the levels of AKT isoforms in *Akt1*$^{+/-}$ *Ptch1*$^{+/-}$ mice and *Ptch1*$^{+/-}$ littermates, assessed by Western blotting. 50 μg protein per lane, actin as an internal control. Brain, brain extracts from *Akt1*$^{+/-}$ *Ptch1*$^{+/-}$.

Genetic ablation of *Akt1* prevents the spontaneous growth of BCCs in *Akt1*$^{+/-}$ *Ptch1*$^{+/-}$mice

There are three known *Akt* isoforms, including *Akt1*, *Akt2*, and *Akt3*. *Akt1*-null mice manifest growth retardation (33), whereas *Akt2*-null mice display an insulin-resistant, diabetes-like syndrome (34), and *Akt3* null mice show impaired brain development (35). Because *Akt1* and *Akt2*, but not *Akt3*, are expressed in the skin, and because mouse embryo fibroblasts lacking *Akt1* (*Akt1*$^{-/-}$ MEF) are sensitive to UV-induced apoptosis (33), we next assessed the effects of *Akt1* deletion in *Ptch1*$^{+/-}$ mice. This study utilized *Akt1* haplodeficient *Ptch1*$^{+/-}$ mice, as *Akt1*$^{-/-}$ littermates rarely survive. The few that do show severe growth retardation and high perinatal mortality (data not shown). Similar to BCNS patients where BCCs develop spontaneously even in sun-protected areas, spontaneous microscopic BCCs were detectable in our *Ptch1*$^{+/-}$ mice starting as early as 8 weeks of age with 100% tumor incidence (ref. 26; Fig. 2). Figure 2A shows representative pictures of histological sections of skin from *Ptch1*$^{+/-}$ and *Akt1*$^{+/-}$ *Ptch1*$^{+/-}$ mice at 12 months of age. *Ptch1*$^{+/-}$ mice carry the insertion of a promoterless lacZ–neo fusion gene, thereby deleting a portion of exon 1 and all of exon 2 of *Ptch1*. Therefore, lacZ activity, mimicking an expression pattern of endogenous Hh target genes (e.g., *Ptch1*), serves as an accurate indicator of Hh pathway activation. In *Ptch1*$^{+/-}$ mice, BCCs were detected by β-gal staining (red arrowheads) with an inset showing a magnified view of an area with multiple BCCs (Fig. 2A, b′). *Akt1* haplodeficiency resulted in substantial reductions in the tumor burden (in both size and number) of spontaneous BCCs in *Akt1*$^{+/-}$ *Ptch1*$^{+/-}$ mice as compared with their *Akt1* WT *Ptch1*$^{+/-}$ littermates (Fig. 2B). Despite isoform-specific functions, it has been shown that *Akt1* knockdown can, in some instances, upregulate and activate AKT2, which in turn compensates for *Akt1* loss (36). Our analysis of *Akt1*$^{+/-}$ *Ptch1*$^{+/-}$ mice shows that AKT2 levels are no different than those in *Ptch1*$^{+/-}$ mice (Fig. 2C), indicating non-overlapping roles for this *AKT* isoform and that AKT1 is crucial for the development of spontaneous BCCs in *Ptch1*$^{+/-}$ mice.

SMO inhibition suppresses AKT1 signaling *in vitro* and *in vivo*

Itraconazole is an FDA-approved azole antifungal drug recently shown to be a potent, and specific inhibitor of Hh signaling (37). It is thought to reduce SMO translocation to the cilium (38). Treatment of murine ASZ001 cells (derived from BCCs induced in B6-*Ptch1*$^{+/-}$) with itraconazole (1–30 μmol/L) dose dependently inhibited the growth of these cells (data not shown) and decreased the levels of the Hh components GLI1, GLI2, and cyclin D1 (Fig. 3A). Interestingly, itraconazole treatment decreased S473 phosphorylation (Fig. 3A). Cyclopamine, a natural compound known to block Hh signaling by binding to SMO, also suppressed

Published OnlineFirst July 7, 2016; DOI: 10.1158/1940-6207.CAPR-16-0066

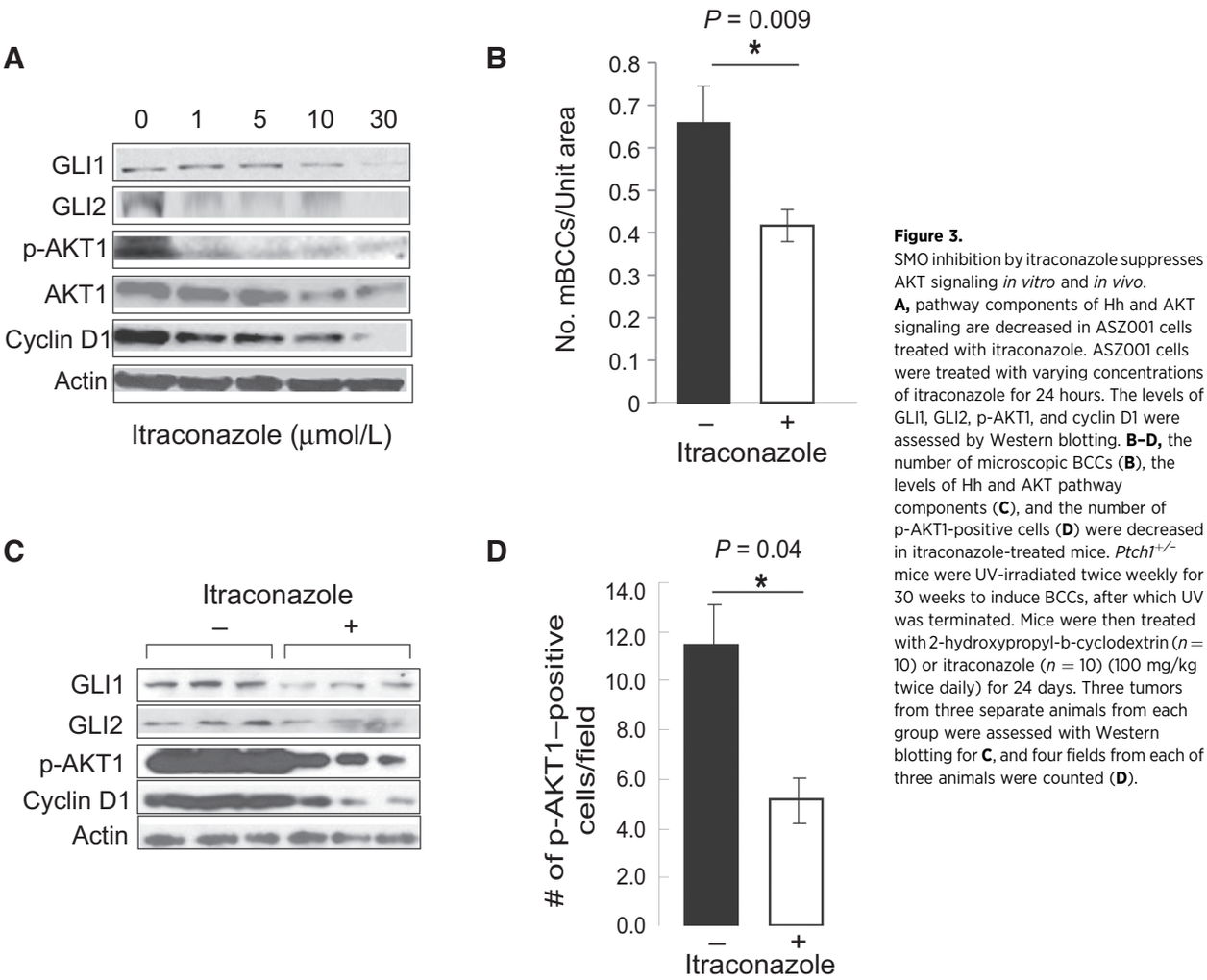

Figure 3.
SMO inhibition by itraconazole suppresses AKT signaling *in vitro* and *in vivo*. **A,** pathway components of Hh and AKT signaling are decreased in ASZ001 cells treated with itraconazole. ASZ001 cells were treated with varying concentrations of itraconazole for 24 hours. The levels of GLI1, GLI2, p-AKT1, and cyclin D1 were assessed by Western blotting. **B–D,** the number of microscopic BCCs (**B**), the levels of Hh and AKT pathway components (**C**), and the number of p-AKT1-positive cells (**D**) were decreased in itraconazole-treated mice. *Ptch1*$^{+/-}$ mice were UV-irradiated twice weekly for 30 weeks to induce BCCs, after which UV was terminated. Mice were then treated with 2-hydroxypropyl-b-cyclodextrin (n = 10) or itraconazole (n = 10) (100 mg/kg twice daily) for 24 days. Three tumors from three separate animals from each group were assessed with Western blotting for **C**, and four fields from each of three animals were counted (**D**).

AKT phosphorylation (data not shown). Oral administration of itraconazole (100 mg/kg twice daily for 24 days) suppressed the growth of existing UV-induced microscopic BCCs in *Ptch1*$^{+/-}$ mice (Fig. 3B) and decreased Hh signaling, AKT phosphorylation, and the number of p-AKT-positive cells in tumors harvested from these animals (Fig. 3C and D). Taken together, these data indicate that AKT signaling is downstream of the Hh pathway.

Akt1 haplodeficiency prevents UV-induced BCC growth in *Ptch1*$^{+/-}$ mice

UV exposure is the major known risk factor for the induction of BCCs, both sporadically in the general population and in BCNS patients (39). Chronic UV irradiation of WT *Ptch1*$^{+/+}$ mice induces the growth of SCCs (Fig. 4A, WT, red arrowheads; Fig. 4B), and these animals were largely resistant to the development of BCCs, as indicated by the absence of β-gal staining (Fig. 4A, WT). In *Ptch1*$^{+/-}$ skin, chronic UV exposure resulted in extensive epidermal hyperplasia (*Ptch1*$^{+/-}$in Fig. 2A vs. Fig. 4A) and greatly enhanced the number and size of BCCs (Fig. 4A, *Ptch1*$^{+/-}$, black arrowheads). *Akt1* haplodeficiency, however, substantially reduced the development of UV-induced BCCs in *Ptch1*$^{+/-}$ mice (Fig. 4C). Extensive colocalization of p-AKT1 S473 with other known BCC markers, GLI1 and SOX9, indicated their concurrent activation in *Ptch1*$^{+/-}$ BCCs (Fig. 4D, *d* and *g*), compared with apparent reductions in AKT S473 phosphorylation and colocalization in *Akt1*$^{+/-}$ *Ptch1*$^{+/-}$ BCCs (Fig. 4D, *i*, *l*, and *o*). These data, together with substantial decreases in KI67, a cell proliferation marker, in *Akt1*$^{+/-}$ *Ptch1*$^{+/-}$ BCCs (Fig. 4D, *c* vs. *k*) further confirmed the importance of AKT1 in BCC growth.

Pharmacological inhibition of AKT inhibits UV-induced BCC growth

We next utilized a battery of AKT inhibitors that are currently in active clinical trials for various other human cancers to assess pharmacologic effects in ASZ001 murine BCC cells. These include the alkyl phospholipid perifosine and MK-2206, an allosteric inhibitor that binds to and inhibits AKT in a non-ATP competitive manner. Perifosine, in particular, has been shown to be relatively nontoxic and well tolerated in phase I/II clinical trials in patients with head and neck SCCs (40–42). Our results indicate that perifosine has a lower IC_{50} for AKT (4 μmol/L) in ASZ001 cells as compared with other inhibitors, which had IC_{50} values ranging up to 50 μmol/L (data not shown). Accordingly, we selected a concentration of 4 μmol/L for further

Published OnlineFirst July 7, 2016; DOI: 10.1158/1940-6207.CAPR-16-0066

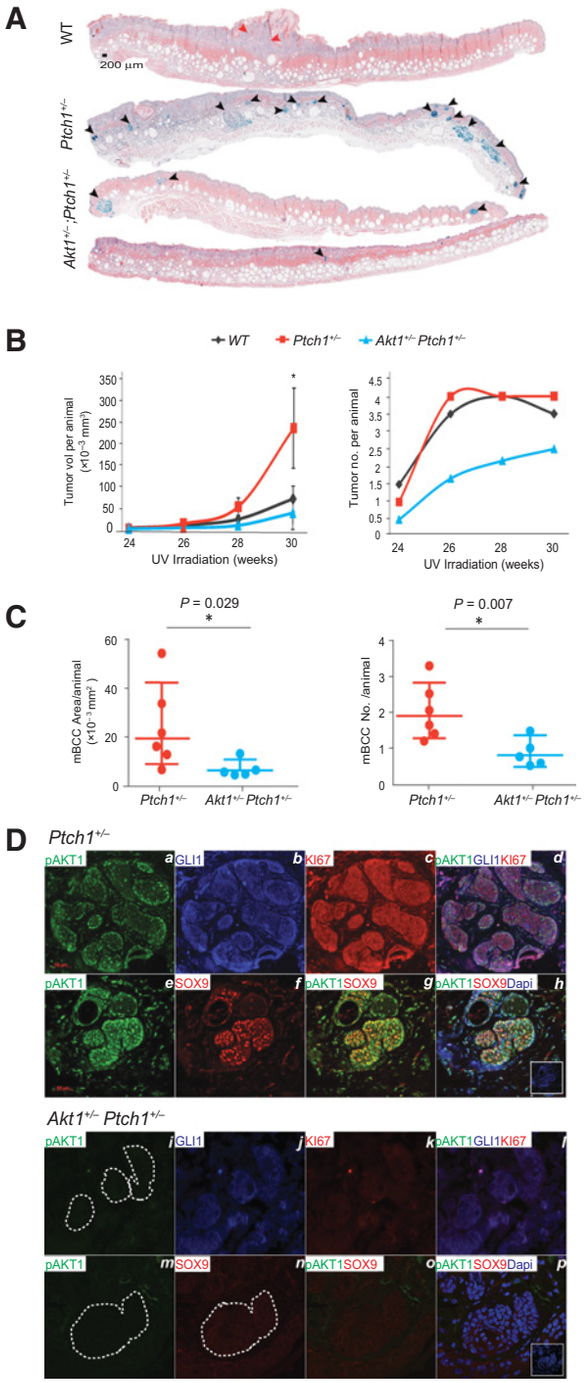

Figure 4.

Haplodeficient *Akt1* suppresses UV-induced BCC tumorigenesis in *Ptch1*$^{+/-}$mice. *Ptch1*$^{+/-}$ ($n = 6$) and *Akt1*$^{+/-}$ *Ptch1*$^{+/-}$($n = 5$), and their WT littermates ($n = 6$) were irradiated with UV (180 mJ/cm^2, twice weekly) for 30 weeks. **A,** representative H&E staining of skin sections harvested at week 30. *Akt1* deficiency suppresses the growth of UV-induced skin tumors (**B**) and microscopic BCCs (**C**). Each dot in **C** represents data from one mouse. Three skin strips (avg. 1.5 cm x 0.1 cm) were analyzed for each mouse. *, $P < 0.005$. **D,** colocalization of p-AKT with GLI1 and KI67, and with SOX9 in UV-induced BCCs in *Ptch1*$^{+/-}$ (*a* – *h*) and *Akt1*$^{+/-}$ *Ptch1*$^{+/-}$(*i* – *p*), as detected by immunofluorescence staining. Magnification, ×40.

studies. Treatment of ASZ001 cells with perifosine, and its alkyl-lysophospholipid analogues, edelfosine, and MK-2206 inhibited AKT S473 and T308 phosphorylations (Fig. 5A). This was associated with substantially reduced proliferation of the ASZ001 cells as assessed by BrdUrd incorporation after 24 hours of treatment with 4 μmol/L of each AKT inhibitor (Fig. 5B). More significantly, only perifosine and edelfosine induced apoptosis in ASZ001 cells, as shown by an increase in cleaved caspase-3 (Fig. 5A, left). Overexpression of myrAKT protected ASZ001 cells from perifosine-induced apoptosis, as shown by decreased levels of caspase-3 (Fig. 5A, right). While MK-2206 reduced p-AKT phosphorylation to levels comparable with that of perifosine or edelfosine (Fig. 5A), it did not affect the proliferative capacity of ASZ001 cells, at least up to a dose of 4 μmol/L. Treatment with MK-2206 for 5 days still showed substantial amounts of EdU incorporation, indicative of cells in the S phase (Fig. 5C, *g*). In contrast, both perifosine and edelfosine completely abolished the proliferative capacity of these cells (Fig. 5C, *e* and *f*), and substantially decreased cell numbers (Fig. 5C, *l* and *m*). Perifosine appears to have superior efficacy in ASZ001 cells, as EdU-positive cells were barely detectable at day 2 (Fig. 5C, *b*). We, therefore, conducted a proof-of-concept preclinical investigation by administering perifosine orally (125 mg/kg, twice weekly) to chronically UV-irradiated *Ptch1*$^{+/-}$ mice for 32 weeks. This regimen significantly reduced total tumor burden (Fig. 5D) as well as the size and number of microscopic BCCs (Fig. 5E). Our results demonstrate the potential utility of targeting AKT signaling to reduce tumor burden in human subjects who are at increased risk for BCC growth.

Discussion

In our previously published investigator-originated clinical trial, we showed that oral administration of the Hh pathway inhibitor vismodegib led to a dramatic reduction in the number of BCCs in BCNS patients, confirming the importance of Hh signaling in driving BCC pathogenesis. However, it soon became apparent in these patients that many of the BCCs that were no longer visible clinically and histologically rapidly recurred after drug discontinuation (9). These results while disappointing do raise intriguing questions regarding the source of the recurrent tumor cells and the mechanisms underlying their regrowth. Moreover, it is known that tumor resistance to vismodegib usually results from SMO mutations that block drug binding and/or reactivate Hh signaling (11, 12). These data collectively suggest that treatment with the currently available inhibitors of Hh signaling is unlikely to permanently eradicate BCCs, and that identification of additional tumor driver pathways distinct from the Hh pathway could lead to the development of innovative therapeutic approaches and could improve clinical outcomes.

Aberrant Akt activation is known to occur frequently in numerous types of human tumors, including those of the skin (16, 18, 19). BCNS patients develop a few to hundreds of BCCs, which in many cases grow aggressively, and may require multiple mutilating surgical procedures. In particular, spontaneous development of multiple BCCs in sun-protected skin is decidedly uncommon in the general human population, but is often a characteristic feature of BCNS patients. Except for the Hh pathway, the mechanisms underlying spontaneous tumor growth are largely unexplored, in

Published OnlineFirst July 7, 2016; DOI: 10.1158/1940-6207.CAPR-16-0066

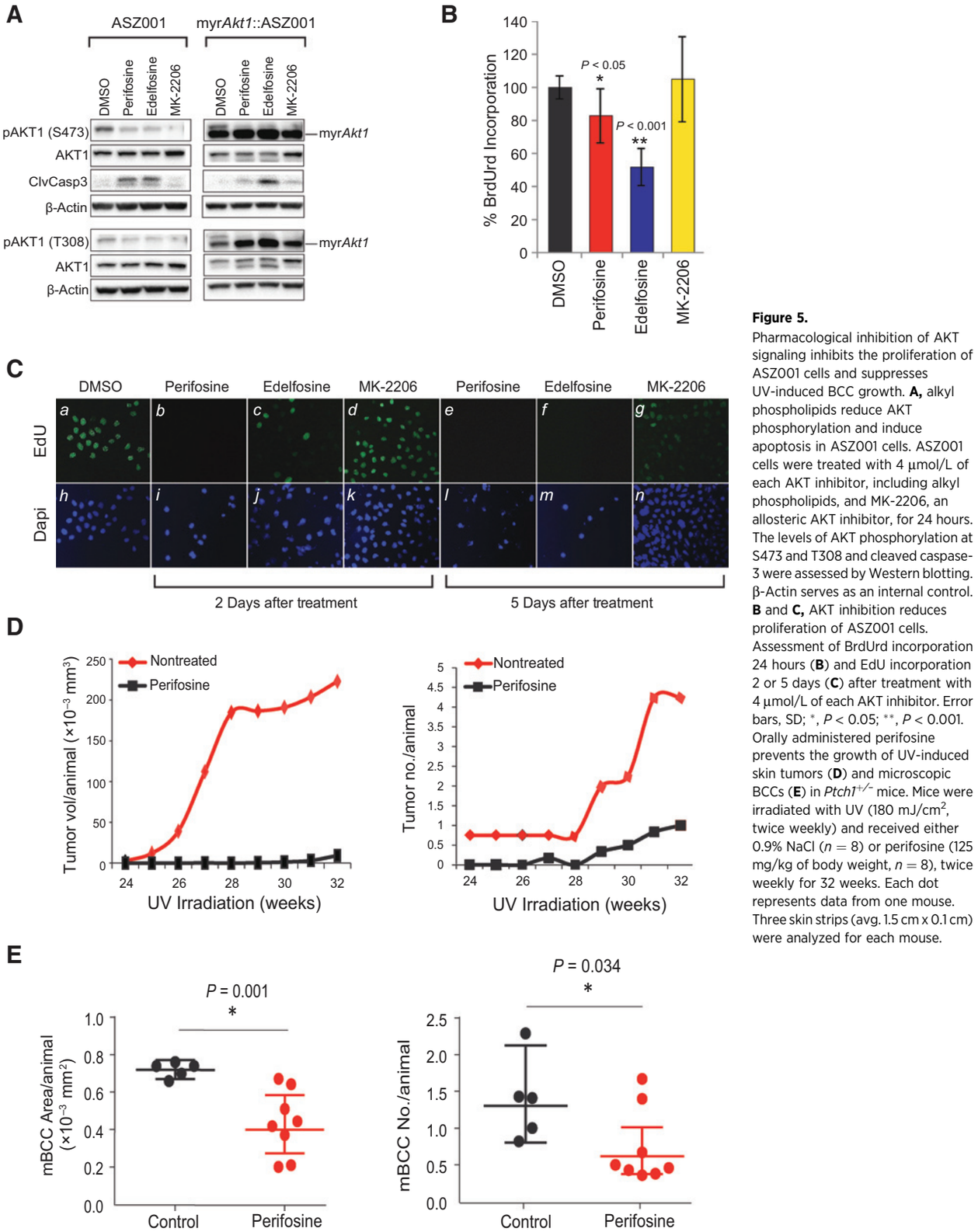

Figure 5.

Pharmacological inhibition of AKT signaling inhibits the proliferation of ASZ001 cells and suppresses UV-induced BCC growth. **A,** alkyl phospholipids reduce AKT phosphorylation and induce apoptosis in ASZ001 cells. ASZ001 cells were treated with 4 μmol/L of each AKT inhibitor, including alkyl phospholipids, and MK-2206, an allosteric AKT inhibitor, for 24 hours. The levels of AKT phosphorylation at S473 and T308 and cleaved caspase-3 were assessed by Western blotting. β-Actin serves as an internal control. **B** and **C,** AKT inhibition reduces proliferation of ASZ001 cells. Assessment of BrdUrd incorporation 24 hours (**B**) and EdU incorporation 2 or 5 days (**C**) after treatment with 4 μmol/L of each AKT inhibitor. Error bars, SD; *, $P < 0.05$; **, $P < 0.001$. Orally administered perifosine prevents the growth of UV-induced skin tumors (**D**) and microscopic BCCs (**E**) in *Ptch1*$^{+/-}$ mice. Mice were irradiated with UV (180 mJ/cm^2, twice weekly) and received either 0.9% NaCl ($n = 8$) or perifosine (125 mg/kg of body weight, $n = 8$), twice weekly for 32 weeks. Each dot represents data from one mouse. Three skin strips (avg. 1.5 cm x 0.1 cm) were analyzed for each mouse.

Published OnlineFirst July 7, 2016; DOI: 10.1158/1940-6207.CAPR-16-0066

part due to the lack of suitable animal models. SKH1-*Ptch1*$^{+/-}$ mice are uniquely susceptible to the development of both spontaneous and UV-induced BCCs, thereby providing an animal model with features that closely resemble those of patients with BCNS. This study directly assessed the effects of *Akt1* loss by introducing *Akt1* haplodeficiency in SKH1-*Ptch1*$^{+/-}$ mice, and demonstrated that *Akt1* is essential for spontaneous BCC tumorigenesis. The absence of AKT S473 phosphorylation, indicative of the lack of its activity, was confirmed in *Akt1*$^{+/-}$ *Ptch1*$^{+/-}$ mice. The concomitant decreased levels of KI67, a marker of proliferation, and tumor burden in these mice further emphasize the importance of AKT1 function in cell survival and proliferation. UV and ionizing radiation are known to exacerbate BCC tumor burden in BCNS patients. The remarkable preclinical efficacy against UV-induced BCCs in *Ptch1*$^{+/-}$ mice of the AKT inhibitor perifosine, selected over other inhibitors based on our *in vitro* studies, indicated that AKT could be an alternative viable target for reducing tumor burden in patients with BCNS.

Akt activation is posttranslational and is mediated through the upstream kinase cascade (e.g., phosphoinositide-dependent kinase 1 [PDK1]) in response to various growth factors and external stimuli. With respect to the Hh pathway, the activation of epidermal growth factor receptor (EGFR), platelet-derived growth factor receptor (PDGFR), and their downstream effectors (e.g., RAS/RAF/MEK/ERK and PI3K/AKT) has been shown to enhance GLI stability and transcriptional activity in various cancers (e.g., chronic lymphocytic leukemia, gastric cancer, and melanoma; refs. 43–47). AKT-mediated GLI activation has also been linked to drug resistance in breast cancer cells (48). While these data position AKT activation upstream of the Hh pathway, reciprocal regulation is also possible. Notably, GLI has been shown to transcriptionally regulate AKT1 expression in diffuse large B-cell lymphoma cells (49), and GLI-mediated AKT and c-MET phosphorylation was recently shown to promote migration and invasion of thyroid tumor cells (50). Our data, demonstrating *in vitro* and *in vivo* inhibition of AKT phosphorylation by the SMO inhibitor itraconazole, also imply that AKT acts downstream of Hh in BCC. In addition, despite the absence of external stimuli, AKT1 phosphorylation levels were significantly elevated in postnatal *Ptch1*$^{+/-}$ keratinocytes compared with *Ptch1* WT keratinocytes, suggesting the existence of intrinsic mechanisms driving AKT phosphorylation. Elevated EGFR levels were previously reported in human BCCs, and forced expression of EGFR and GLI was shown to be critical for oncogenic transformation of spontaneously transformed, non-tumorigenic HaCaT keratinocytes (51, 52). However, EGFR levels, as well as PDGFR, were barely detectable, and no apparent differences were observed in p-MEK1/2 levels, regardless of *Ptch1* status (data not shown). These results strongly suggest the lack of involvement of EGFR signaling in AKT phosphorylation in *Ptch1*$^{+/-}$ keratinocytes; however, the exact mechanisms await further investigation. In addition, while GLI1 levels remained somewhat similar in UV-induced BCCs, irrespective of *Akt1* status, the apparent reduction in SOX9 levels in *Akt1*$^{+/-}$ BCCs raises interesting questions with regard to the targets of AKT1 and its relevance to Hh signaling and BCC pathogenesis. Integration of the AKT and Hh pathways is undoubtedly under the influence of multiple regulatory pathways, which may account for the specificity and tumorigenic susceptibility of different target cells. Further investigation will likely reveal additional novel mechanism-driven targets for the chemoprevention and treatment of this most common type of human malignancy.

Disclosure of Potential Conflicts of Interest

D.R. Bickers is a consultant/advisory board member for SC Johnson Co. and has received an expert testimony from Goodwin Proctor LLP. No potential conflicts of interest were disclosed by the other authors.

Authors' Contributions

Conception and design: A.L. Kim, M. Athar, D.R. Bickers
Development of methodology: A.L. Kim, J.H. Back, Y. Zhu, D.R. Bickers
Acquisition of data (provided animals, acquired and managed patients, provided facilities, etc.): A.L. Kim, J.H. Back, Y. Zhu, X. Tang, N.P. Yardley, D.R. Bickers
Analysis and interpretation of data (e.g., statistical analysis, biostatistics, computational analysis): A.L. Kim, J.H. Back, Y. Zhu, N.P. Yardley, D.R. Bickers
Writing, review, and/or revision of the manuscript: A.L. Kim, N.P. Yardley, K.J. Kim, M. Athar, D.R. Bickers
Administrative, technical, or material support (i.e., reporting or organizing data, constructing databases): A.L. Kim, X. Tang, K.J. Kim, D.R. Bickers
Study supervision: A.L. Kim, M. Athar

Grant Support

This work was partially supported by the NIH Grants (R01-ES-020344 to D.R. Bickers, and R01 CA138998 to M. Athar) and Irving Scholar Award to A.L. Kim.

The costs of publication of this article were defrayed in part by the payment of page charges. This article must therefore be hereby marked advertisement in accordance with 18 U.S.C. Section 1734 solely to indicate this fact.

Received March 2, 2016; revised June 8, 2016; accepted June 28, 2016; published OnlineFirst July 7, 2016.

References

1. Briscoe J, Therond PP. The mechanisms of Hedgehog signalling and its roles in development and disease. Nat Rev Mol Cell Biol 2013;14:416–29.
2. Kar S, Deb M, Sengupta D, Shilpi A, Bhutia SK, Patra SK. Intricacies of hedgehog signaling pathways: a perspective in tumorigenesis. Exp Cell Res 2012;318:1959–72.
3. Athar M, Li C, Kim AL, Spiegelman VS, Bickers DR. Sonic hedgehog signaling in Basal cell nevus syndrome. Cancer Res 2014;74:4967–75.
4. Robbins DJ, Fei DL, Riobo NA. The hedgehog signal transduction network. Sci Signal 2012;5:re6-.
5. Jenkins D.Hedgehog signalling: emerging evidence for non-canonical pathways. Cell Signal 2009;21:1023–34.
6. Gupta S, Takebe N, Lorusso P. Targeting the Hedgehog pathway in cancer. Thera Adv Med Oncol 2010;2:237–50.
7. Miller DL, Weinstock MA. Nonmelanoma skin cancer in the United States: incidence. J Am Acad Dermatol 1994;30:774–8.
8. Gorlin RJ.Nevoid basal-cell carcinoma syndrome. Medicine 1987;66:98–113.
9. Tang JY, Mackay-Wiggan JM, Aszterbaum M, Yauch RL, Lindgren J, Chang K, et al. Inhibiting the hedgehog pathway in patients with the basal-cell nevus syndrome. N Eng J Med 2012;366:2180–8.
10. Atwood SX, Chang AL, Oro AE. Hedgehog pathway inhibition and the race against tumor evolution. J Cell Biol 2012;199:193–7.
11. Sharpe HJ, Pau G, Dijkgraaf GJ, Basset-Seguin N, Modrusan Z, Januario T, et al. Genomic analysis of smoothened inhibitor resistance in Basal cell carcinoma. Cancer Cell 2015;27:327–41.
12. Atwood SX, Sarin KY, Whitson RJ, Li JR, Kim G, Rezaee M, et al. Smoothened variants explain the majority of drug resistance in Basal cell carcinoma. Cancer Cell 2015;27:342–53.

Published OnlineFirst July 7, 2016; DOI: 10.1158/1940-6207.CAPR-16-0066

13. Pricl S, Cortelazzi B, Dal Col V, Marson D, Laurini E, Fermeglia M, et al. Smoothened (SMO) receptor mutations dictate resistance to vismodegib in basal cell carcinoma. Mol Oncol 2015;9:389–97.
14. Kasper M, Jaks V, Hohl D, Toftgard R. Basal cell carcinoma - molecular biology and potential new therapies. J Clin Invest 2012;122:455–63.
15. Bonilla X, Parmentier L, King B, Bezrukov F, Kaya G, Zoete V, et al. Genomic analysis identifies new drivers and progression pathways in skin basal cell carcinoma. Nat Genet 2016;48:398–406.
16. Hay N.The Akt-mTOR tango and its relevance to cancer. Cancer Cell 2005;8:179–83.
17. Porta C, Paglino C, Mosca A. Targeting PI3K/Akt/mTOR signaling in cancer. Front Oncol 2014;4:64.
18. Crowell JA, Steele VE, Fay JR. Targeting the AKT protein kinase for cancer chemoprevention. Mol Cancer Therapeut 2007;6:2139–48.
19. Ming M, He Y-Y. PTEN: new insights into its regulation and function in skin cancer. J Invest Dermatol 2009;129:2109–12.
20. Guertin DA, Sabatini DM. Defining the role of mTOR in cancer. Cancer Cell 2007;12:9–22.
21. Aszterbaum M, Epstein J, Oro A, Douglas V, LeBoit PE, Scott MP, et al. Ultraviolet and ionizing radiation enhance the growth of BCCs and trichoblastomas in patched heterozygous knockout mice. Nat Med 1999;5:1285–91.
22. So P-L, Langston AW, Daniallinia N, Hebert JL, Fujimoto MA, Khaimskiy Y, et al. Long-term establishment, characterization and manipulation of cell lines from mouse basal cell carcinoma tumors. Exp Dermatol 2006; 15:742–50.
23. Aszterbaum M, Rothman A, Johnson RL, Fisher M, Xie J, Bonifas JM, et al. Identification of mutations in the human PATCHED gene in sporadic basal cell carcinomas and in patients with the basal cell nevus syndrome. J Invest Dermatol 1998;110:885–8.
24. Kim AL, Athar M, Bickers DR, Gautier J. Ultraviolet-B-induced G1 arrest is mediated by downregulation of cyclin-dependent kinase 4 in transformed keratinocytes lacking functional p53. J Invest Dermatol 2002;118:818–24.
25. Kim AL, Athar M, Bickers DR, Gautier J. Stage-specific alterations of cyclin expression during UVB-induced murine skin tumor development. Photochem Photobiol 2002;75:58–67.
26. Chaudhary SC, Tang X, Arumugam A, Li C, Srivastava RK, Weng Z, et al. Shh and p50/Bcl3 signaling crosstalk drives pathogenesis of BCCs in Gorlin syndrome.Oncotarget 2015;6:36789–814.
27. Goodrich LV, Milenkovic L, Higgins KM, Scott MP. Altered neural cell fates and medulloblastoma in mouse patched mutants. Science 1997;277: 1109–13.
28. Tang X, Kim AL, Feith DJ, Pegg AE, Russo J, Zhang H, et al. Ornithine decarboxylase is a target for chemoprevention of basal and squamous cell carcinomas in Ptch1$^{+/-}$ mice. J Clin Invest 2004;113:867–75.
29. Aszterbaum M, Epstein J, Oro A, Douglas V, LeBoit PE, Scott MP, et al. Ultraviolet and ionizing radiation enhance the growth of BCCs and trichoblastomas in patched heterozygous knockout mice. Nat Med 1999;5:1285–91.
30. Brash DE, Rudolph JA, Simon JA, Lin A, McKenna GJ, Baden HP, et al. A role for sunlight in skin cancer: UV-induced p53 mutations in squamous cell carcinoma. Proc Natl Acad Sci USA 1991;88:10124–8.
31. Xu J, Athar M, Kopelovich L. Abstract 4202: Hair follicles disruption leads to enhanced UVB-induced cutaneous inflammation and basal cell carcinoma development. Cancer Res 2011;71:4202.
32. Sarbassov DD, Guertin DA, Ali SM, Sabatini DM. Phosphorylation and regulation of Akt/PKB by the rictor-mTOR complex. Science 2005;307: 1098–101.
33. Chen WS, Xu P-Z, Gottlob K, Chen M-L, Sokol K, Shiyanova T, et al. Growth retardation and increased apoptosis in mice with homozygous disruption of the akt1 gene. Gen Develop 2001;15:2203–8.
34. Cho H, Mu J, Kim JK, Thorvaldsen JL, Chu Q, Crenshaw EB, et al. Insulin resistance and a diabetes mellitus-like syndrome in mice lacking the protein kinase Akt2 (PKBβ). Science 2001;292:1728–31.
35. Gonzalez E, McGraw TE. The Akt kinases: isoform specificity in metabolism and cancer. Cell cycle (Georgetown, Tex) 2009;8:2502–8.
36. Zhang L, Sun S, Zhou J, Liu J, Lv JH, Yu XQ, et al. Knockdown of akt1 promotes akt2 upregulation and resistance to oxidative-stress-induced apoptosis through control of multiple signaling pathways. Antioxid Redox Sig 2011;15:1–17.
37. Kim J, Tang JY, Gong R, Kim J, Lee JJ, Clemons KV, et al. Itraconazole, a commonly used antifungal that inhibits Hedgehog pathway activity and cancer growth. Cancer Cell 2010;17:388–99.
38. Amakye D, Jagani Z, Dorsch M. Unraveling the therapeutic potential of the Hedgehog pathway in cancer. Nat Med 2013;19:1410–22.
39. Gorlin RJ.Nevoid basal cell carcinoma (Gorlin) syndrome. Genet Med 2004;6:530–9.
40. Ghobrial IM, Roccaro A, Hong F, Weller E, Rubin N, Leduc R, et al. Clinical and translational studies of a phase II trial of the novel oral Akt inhibitor perifosine in relapsed or relapsed/refractory Waldenstrom's macroglobulinemia. Clin Cancer Res 2010;16:1033–41.
41. LoPiccolo J, Blumenthal GM, Bernstein WB, Dennis PA. Targeting the PI3K/Akt/mTOR pathway: effective combinations and clinical considerations. Drug Resist Updat 2008;11:32–50.
42. Gills JJ, Dennis PA. Perifosine: update on a novel Akt inhibitor. Curr Oncol Rep 2009;11:102–10.
43. Kern D, Regl G, Hofbauer SW, Altenhofer P, Achatz G, Dlugosz A, et al. Hedgehog/GLI and PI3K signaling in the initiation and maintenance of chronic lymphocytic leukemia. Oncogene 2015;34: 5341–51.
44. Kasper M, Schnidar H, Neill GW, Hanneder M, Klingler S, Blaas L, et al. Selective modulation of hedgehog/GLI target gene expression by epidermal growth factor signaling in human keratinocytes. Mol Cell Biol 2006; 26:6283–98.
45. Stecca B, Mas C, Clement V, Zbinden M, Correa R, Piguet V, et al. Melanomas require HEDGEHOG-GLI signaling regulated by interactions between GLI1 and the RAS-MEK/AKT pathways. Proc Natl Acad Sci 2007;104:5895–900.
46. Pelczar P, Zibat A, van Dop WA, Heijmans J, Bleckmann A, Gruber W, et al. Inactivation of patched1 in mice leads to development of gastrointestinal stromal-like tumors that express Pdgfrα but not kit. Gastroenterology 2013;144:134–44.e6.
47. Riobó NA, Lu K, Ai X, Haines GM, Emerson CP. Phosphoinositide 3-kinase and Akt are essential for Sonic Hedgehog signaling. Proc Natl Acad Sci USA 2006;103:4505–10.
48. Das S, Samant RS, Shevde LA. Nonclassical activation of hedgehog signaling enhances multidrug resistance and makes cancer cells refractory to smoothened-targeting hedgehog inhibition. J Biol Chem 2013;288: 11824–33.
49. Agarwal NK, Qu C, Kunkulla K, Liu Y, Vega F. Transcriptional regulation of serine/threonine protein kinase (AKT) genes by glioma-associated oncogene homolog 1. J Biol Chem 2013;288:15390–401.
50. Williamson AJ, Doscas ME, Ye J, Heiden KB, Xing M, Li Y, et al. The sonic hedgehog signaling pathway stimulates anaplastic thyroid cancer cell motility and invasiveness by activating Akt and c-Met. Oncotarget 2016; 7:10472–85.
51. Schnidar H, Eberl M, Klingler S, Mangelberger D, Kasper M, Hauser-Kronberger C, et al. Epidermal growth factor receptor signaling synergizes with hedgehog/GLI in oncogenic transformation via activation of the MEK/ERK/JUN pathway. Cancer Res 2009;69:1284–92.
52. Krähn G, Leiter U, Kaskel P, Udart M, Utikal J, Bezold G, et al. Coexpression patterns of EGFR, HER2, HER3 and HER4 in non-melanoma skin cancer. Eur J Cancer 2001;37:251–9.

Published OnlineFirst July 7, 2016; DOI: 10.1158/1940-6207.CAPR-16-0066

Cancer Prevention Research

AKT1 Activation is Obligatory for Spontaneous BCC Tumor Growth in a Murine Model that Mimics Some Features of Basal Cell Nevus Syndrome

Arianna L. Kim, Jung Ho Back, Yucui Zhu, et al.

Cancer Prev Res 2016;9:794-802. Published OnlineFirst July 7, 2016.